

# 9

## Regge poles in perturbation theory

### 9.1 Reggeons, ladder graphs, and multiparticle production

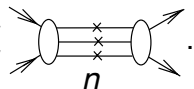
We have studied two-particle reactions and introduced objects of ‘variable spin’ – *reggeons* as a generalization of usual particles. The reggeon amplitude,

$$A_{\text{regg}}^{\pm}(s, q^2) \propto \xi_{\alpha} s^{\alpha}, \quad \xi_{\alpha} = \frac{e^{-i\pi\alpha} \pm 1}{-\sin \pi\alpha}, \quad \alpha = \alpha(q^2),$$

differs essentially from the particle-exchange amplitude,

$$A_{\sigma}(q^2, s) \propto \frac{s^{\sigma}}{\mu^2 - q^2 - i\varepsilon},$$

by a non-trivial complexity, even at  $q^2 < 0$  where particle exchange is real. As the  $s$ -channel unitarity tells us, the imaginary part of the elastic amplitude is determined by real processes, mostly by many-particle production since  $s$  is very large:

$$\text{Im } A_{\text{el}}(s, q^2) \simeq s\sigma_{\text{tot}} = \frac{1}{2} \sum_n \text{Diagram}_n.$$


This means that the reggeon, having a large imaginary part,

$$\text{Im } A_{\text{regg}}^{\pm} \propto \text{Im} \left[ i - \frac{\cos \pi\alpha \pm 1}{\sin \pi\alpha} \right] s^{\alpha} = s^{\alpha},$$

is not an elementary object but is ‘composed’ of certain inelastic  $s$ -channel processes. We have to understand what these processes are.

As we have discussed before, from the point of view of  $t$ -channel dynamics, the Regge pole is a bound state of non-relativistic particles. But

the interaction of slow particles can be described in terms of a potential:

$$\text{Diagram} = \text{Diagram}_1 + \text{Diagram}_2 + \dots + \text{Diagram}_n + \dots \tag{9.1}$$

The potential acts without retardation, therefore the dashed lines do not cross. If it turns out that indeed, the reggeon corresponds to potential scattering in the  $t$ -channel, this would answer the question which inelastic processes are important at high energies. Cutting through the diagrams on the r.h.s. of (9.1) we obtain *ladders* as an image of inelastic processes ‘describing’ the reggeon.

$$\text{Im } A_{\text{regg}} \sim \sum \text{Diagram} . \tag{9.2}$$

These are processes of production of a large number of particles, those very particles that play the rôle of the binding potential in the crossing channel.

### 9.2 Reggeization in $g\phi^3$ theory

In order to verify that the sum of the diagrams (9.1) gives rise to a Regge behaviour,

$$A = b(t) s^{\alpha(t)}, \tag{9.3}$$

we will address the problem perturbatively and employ the simplest  $g\phi^3$  theory with a small coupling. Although this quantum field theory is far from realistic, this academic exercise will teach us important lessons about the phenomenon of *reggeization*. Later we will try to generalize the results beyond the perturbation theory.

#### 9.2.1 Qualitative analysis of higher order diagrams

We are going to construct perturbation theory for the elastic amplitude in the relevant region of the Mandelstam plane:

$$s \simeq -u \rightarrow \infty, \quad |t| \sim m^2.$$

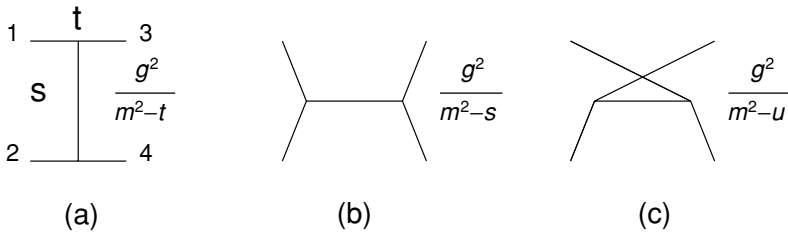
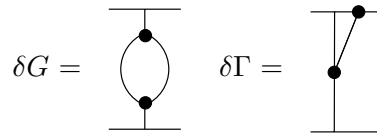


Fig. 9.1 Born diagrams for  $A(1, 2 \rightarrow 3, 4)$  in  $g\phi^3$  theory.

We start from the Born approximation. Of the Born graphs Fig. 9.1, the first one is  $\mathcal{O}(g^2/m^2)$  and dominates the asymptotics, while the graphs Fig. 9.1(b) and (c) are much smaller at high energies,  $\mathcal{O}(g^2/s)$ . Since the coupling has a dimension of mass, in higher orders of the perturbative expansion each extra power of  $g^2$  is accompanied by  $m^2$ , or  $t \sim m^2$ , or  $s \simeq -u$  in the denominator. To build up the characteristic behaviour (9.3), we need to search for *large* perturbative corrections of the relative size

$$A^{(n+1)}/A^{(n)} \propto \frac{g^2}{m^2} \ln s. \tag{9.4}$$

It is clear that self-energy and vertex insertions into the Born graphs cannot lead to the Regge structure (9.3), since corrections of this type are functions of only one invariant, either  $t$ , or  $s$ .



The theory is convergent in the ultraviolet region, and no corrections may come from the region of large virtual momenta. Therefore only specific diagrams (and for a special reason) may contain the large logarithmic factor (9.4).

In the next order we have three topologically new diagrams of Fig. 9.2. In the last graph, Fig. 9.2(c), all four propagators are large,  $|k_i^2| \sim s$ , making its contributions negligibly small,  $\mathcal{O}(g^4/s^2)$ . The first two diagrams

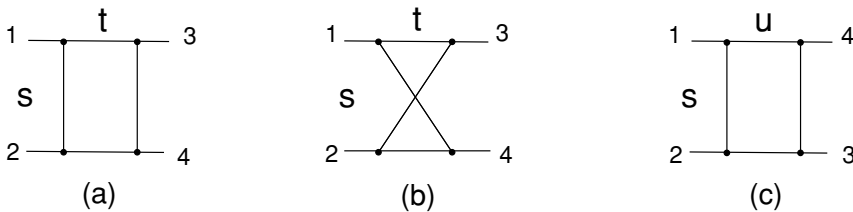


Fig. 9.2 Second-order diagrams.

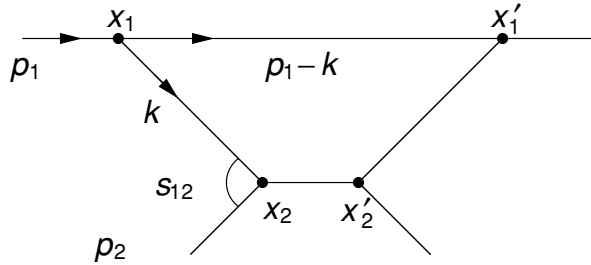


Fig. 9.3 Long-living fluctuation in the rest frame of  $p_2$ .

are much larger and can be considered as  $g^2/m^2$  corrections to the Born graphs Fig. 9.1(b) and (c). It is these two which will interest us. Let us show that they contain the  $\ln s$  enhancement indeed.

9.2.2 Dominance of ladder graphs: space-time picture

In fact we have already considered the diagram Fig. 9.2(a) when we discussed how to make the interaction radius increasing with energy. In Section 5.6 we observed that in the rest frame of the particle  $p_2$  the projectile  $p_1$ , having a very large energy  $p_{10} \simeq s/2m$ , may fluctuate into a pair of particles. We saw that if virtualities of the offspring are limited,  $|k^2| \sim |(p_1 - k)^2| \sim m^2$ , the energy uncertainty turns out to be very small, see (5.60):

$$\Delta E \sim \frac{m^2}{x(1-x)p_{10}} \sim \frac{m^3}{s} \ll m, \quad x = \frac{k_0}{p_{10}}.$$

At high energies large longitudinal distances become important,

$$|x'_1 - x_1| \lesssim \Delta t \sim \frac{1}{\Delta E} \sim \frac{x(1-x)s}{m^3} \gg m^{-1}, \tag{9.5}$$

and the fluctuation may occur long before the projectile hits the target. The origin of the logarithmic growth of our diagram is precisely the integration over large longitudinal distances:

$$\int \frac{e^{i\Delta E(x'_1-x_1)}}{|x'_1 - x_1|} dx'_1 \sim \ln \frac{m}{\Delta E} \sim \ln \frac{s}{m^2}.$$

(The distance between  $x_2$  and  $x'_2$  in Fig. 9.3 stays small.) In order to have a long-living fluctuation, see (9.5), both particles  $k$  and  $(p_1 - k)$  in the decay vertex must be relativistic:  $x, (1-x) \gg m^2/s$ . At the same time, the target prefers to interact with a slower particle, since in the lower vertex in Fig. 9.3 two point-like particles interact in the  $S$ -wave state

with the cross section

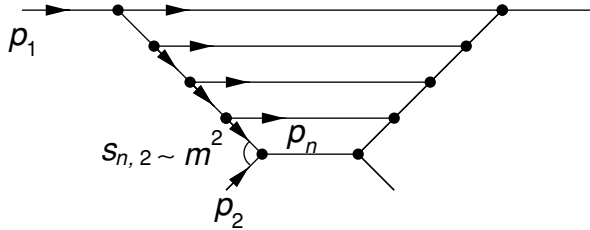
$$\sigma \sim \pi\lambda_c^2 \sim \frac{1}{s_{12}} \simeq \frac{1}{2mk_0} = \frac{1}{xs}.$$

As a result of the interplay of these two tendencies, the amplitude remains small,  $A \sim s^{-1}$ , but acquires a logarithmic enhancement in the next order,

$$A^{(0)}[\text{Fig. 9.1b}] \simeq \frac{g^2}{-s}, \quad A^{(1)}[\text{Fig. 9.2a}] \sim \frac{g^2}{-s} \times \frac{g^2}{m^2} \ln \frac{s}{m^2}.$$

We have a rather curious situation here. We chose a superconvergent theory with a small coupling constant  $g^2/m^2 \ll 1$  and expected that we could rely on the perturbation theory. However, with  $s$  increasing, the incident particle gets more and more time to decay; eventually it will *always* do so, even if the interaction constant is small. But this means that the perturbation theory must fail! And this is exactly what happens: with the increase of  $s$  the *true expansion parameter* (9.4) sooner or later becomes of the order of unity so that *all orders* of the perturbative expansion become equally important.

The virtual particle  $k$  in Fig. 9.3 will decay in its turn, and the process will continue until a relatively slow particle with a momentum  $k_n \sim m$  appears, which interacts with the target with a ‘normal’ cross section  $\sigma \sim m^{-2}$ .

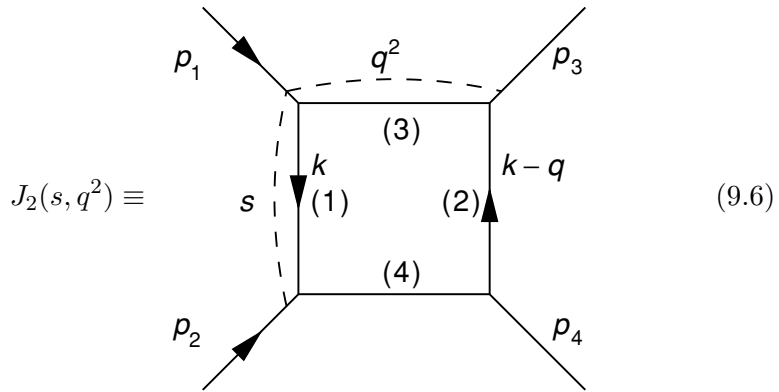


In such a process with  $n$  virtual particles along the decay chain, there are  $n$  independent integrations over the longitudinal distances. Hence, it is natural to expect that the  $n$ th-order correction to the Born graph will be enhanced as  $(\ln s)^n$ . Our hope is that summing up all ladder graphs we will obtain just the Regge amplitude (9.3):

$$+ \dots \stackrel{s \rightarrow \infty}{\simeq} b(t)s^{\alpha(t)}.$$

9.2.3 Calculation of the box diagram

Let us demonstrate how this happens. We begin with the calculation of the behaviour of the diagram of Fig. 9.3 in the kinematical region  $s \gg -q^2 \sim m^2$ . This is the shortest ladder, with two rungs only, so we call it  $J_2$ :



We define the light-like Sudakov momenta

$$(p'_1)^2 = (p'_2)^2 = 0; \quad p'_1 \simeq p_1 - \gamma p_2, \quad p'_2 \simeq p_2 - \gamma p_1; \quad \gamma = \frac{m^2}{s}; \quad s = 2(p'_1 p'_2),$$

to cast the four-vector of the momentum transfer  $q = p_1 - p_3$  as

$$q = \beta_q p'_1 + \alpha_q p'_2 + q_\perp; \quad \alpha_q = \frac{q^2}{s}, \quad \beta_q = -\frac{q^2}{s}. \tag{9.7}$$

Recall that in our high-energy kinematics momentum transfer is ‘transversal’ in the sense of

$$q^2 \simeq (q_\perp)^2 \cdot (1 + \mathcal{O}(s^{-1})).$$

By construction, the four-vector  $q^\mu_\perp$  is orthogonal to  $p^\mu_1$  and  $p^\mu_2$ ; in the reference frames where  $\mathbf{p}_1$  and  $\mathbf{p}_2$  lie on the same line,  $q_\mu$  becomes the usual three-vector perpendicular to this line (collision axis),  $q_\perp = (0; 0, \mathbf{q}_\perp)$ ,

$$q^2 \simeq -\mathbf{q}_\perp^2.$$

Finite-state particles have finite transverse components,  $\mathbf{p}_{4\perp} = -\mathbf{p}_{3\perp} = \mathbf{q}_\perp$ , i.e. particles scatter at a small angle. Then we write

$$k = \beta p'_1 + \alpha p'_2 + k_\perp.$$

Transverse momentum integrals in the  $g\phi^3$  theory converge,  $|k_\perp| \sim m$ , so we will have to look for the logarithmic enhancement in the  $\alpha$ - $\beta$  sector.

Our amplitude reads

$$J_2(s, q^2) = g^4 \int \frac{d^4k}{(2\pi)^4 i} \frac{1}{(1)(2)(3)(4)}, \tag{9.8}$$

where the Feynman denominators are

$$\begin{aligned} (1) &\equiv m^2 - k^2 - i\varepsilon, & (2) &\equiv m^2 - (k-q)^2 - i\varepsilon, \\ (3) &\equiv m^2 - (k-p_1)^2 - i\varepsilon, & (4) &\equiv m^2 - (k+p_2)^2 - i\varepsilon. \end{aligned}$$

We obtain

$$(1) = -\alpha\beta s + m^2 + \mathbf{k}_\perp^2 - i\varepsilon, \tag{9.9a}$$

$$(2) = -(\alpha - \alpha_q)(\beta - \beta_q)s + m^2 + (\mathbf{k} - \mathbf{q})_\perp^2 - i\varepsilon, \tag{9.9b}$$

$$(3) = -(\alpha - \gamma)(\beta - 1)s + m^2 + \mathbf{k}_\perp^2 - i\varepsilon, \tag{9.9c}$$

$$(4) = -(\alpha + 1)(\beta + \gamma)s + m^2 + \mathbf{k}_\perp^2 - i\varepsilon. \tag{9.9d}$$

Loop integration in terms of Sudakov variables has the structure

$$\int d^4k = \frac{s}{2} \int_{-\infty}^{\infty} d\alpha \int_{-\infty}^{\infty} d\beta \int d^2\mathbf{k}_\perp.$$

Let us start from a rough estimate of the magnitude of the answer to get a feeling what we should expect. Dimension-wise, the answer may turn out to be very small if all the virtualities happen to be of the order of  $s$ , the biggest invariant:  $d^4k/(k^2)^4 \sim s^{-2}$ . So we better try to keep all the denominators as small as possible. Given  $k_\perp = \mathcal{O}(m)$ , from (9.9c, d) follows an estimate for the virtualities of the ‘horizontal’ lines,

$$(3) \sim \alpha s, \quad (4) \sim -\beta s. \tag{9.10}$$

$\beta$  is the fraction of the incoming momentum  $p_1$  transferred to the bottom of the diagram (9.6) and, vice versa,  $(-\alpha)$  measures the fraction of  $p_2$  that flows into the top. It looks natural to have  $\beta, (-\alpha) \ll 1$ ; in this case an incident particle passes its large momentum almost entirely to the neighbouring ‘horizontal’ line,  $(p_1 - k) \simeq p_1, (p_2 + k) \simeq p_2$ .

Wanting to keep virtualities (3) and (4) finite, we demand

$$\beta \sim \frac{m^2}{s}, \quad -\alpha \sim \frac{m^2}{s}, \tag{9.11a}$$

in which case the ‘longitudinal parts’ of the ‘vertical’ propagators (9.9a, b) are negligibly small,  $\alpha\beta s \sim m^2/s$ , and (1) and (2) become purely

transversal. Then from the kinematical region (9.11a) we get

$$J_2 \sim \frac{g^4}{s} \int \frac{d^2 \mathbf{k}_\perp}{(1)(2)} \iint \frac{d\alpha d\beta}{(3)(4)} \sim \frac{-g^4}{sm^2} \int \frac{d(\alpha s)}{\alpha s} \int \frac{d(\beta s)}{\beta s} \sim \frac{-g^4}{sm^2}. \quad (9.11b)$$

This is *almost* the correct answer. We can get more if we release the strong restrictions (9.11a) and allow  $\alpha$  and  $\beta$  to vary broader:

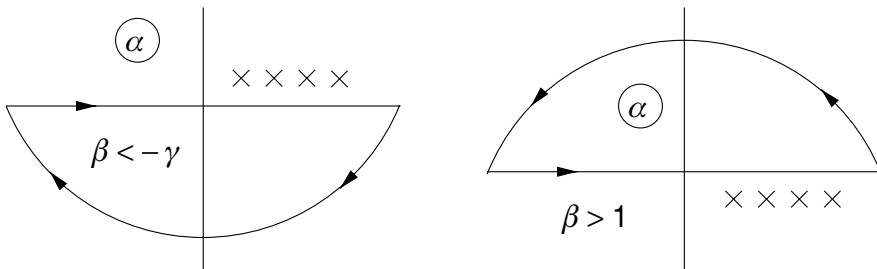
$$\frac{m^2}{s} \ll \beta \ll 1, \quad \frac{m^2}{s} \ll -\alpha \ll 1. \quad (9.11c)$$

The virtual propagators (9.10) then become relatively large but we gain a logarithmic enhancement by integrating over the  $\beta/\alpha$  ratio along the hyperbola  $\alpha\beta s = \text{const}$ .

We are now ready to calculate the amplitude exactly. Take first, e.g. the integral over  $\alpha$ . Since it converges at infinity (as  $d\alpha/\alpha^4$ ), the contour can be closed either in the upper or the lower half-plane, whichever we find more convenient. This simplifies the calculation of the integral by residues. The poles in  $\alpha$  of the integrand are due to four denominators:

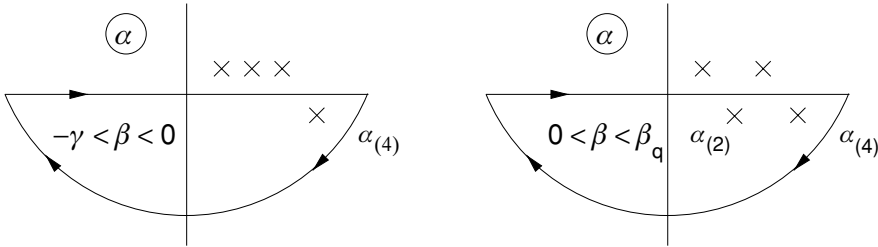
$$\begin{aligned} \alpha_{(1)} &= \frac{m^2 + \mathbf{k}_\perp^2 - i\varepsilon}{\beta s}, & \alpha_{(2)} &= \alpha_q + \frac{m^2 + (\mathbf{q} - \mathbf{k})_\perp^2 - i\varepsilon}{(\beta - \beta_q) s}, \\ \alpha_{(3)} &= \gamma - \frac{m^2 + \mathbf{k}_\perp^2 - i\varepsilon}{(1 - \beta) s}, & \alpha_{(4)} &= -1 + \frac{m^2 + \mathbf{k}_\perp^2 - i\varepsilon}{(\beta + \gamma) s}. \end{aligned} \quad (9.12)$$

In order to choose the best strategy, we have to look at the *imaginary parts* of the poles  $\alpha_{(i)}$  due to Feynman's  $i\varepsilon$ . The configuration of the poles depends on the value of  $\beta$ . First we observe that if  $\beta < -\gamma$  all four poles are situated *above* the real axis. In this case we close the contour in the *lower* half-plane to get zero. Analogously, if  $\beta > 1$  we get the same result by closing the contour *upwards* and leaving all the poles outside the loop, *below* the real axis.

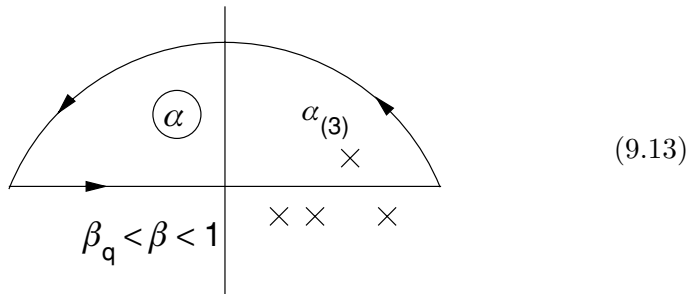


Next, we have two intervals of  $\beta$  where we close the contour on the lower half-plane around one pole,  $\alpha = \alpha_{(4)}$ , and two poles, (2) and (4), correspondingly:





Since both  $\gamma = m^2/s$  and  $\beta_q = -q^2/s$  are very small, these integration intervals in  $\beta$  are tiny and do not produce the  $\ln s$  enhancement we are looking for (cf. (9.11b)). We are left with the large interval  $\beta_q < \beta < 1$ :



This interval gives the main contribution due to the logarithmic integration over  $\beta$  under the conditions

$$\frac{m^2}{s} \ll \beta \ll 1. \tag{9.14}$$

Given these strong inequalities, we estimate  $\alpha = \alpha_{(3)} = \mathcal{O}(m^2/s)$ , the remaining denominators simplify,

$$(1) \simeq m^2 + \mathbf{k}_\perp^2, \tag{9.15a}$$

$$(2) \simeq m^2 + (\mathbf{k} - \mathbf{q})_\perp^2, \tag{9.15b}$$

$$(4) \simeq m^2 + \mathbf{k}_\perp^2 - \beta s - i\varepsilon, \tag{9.15c}$$

and we obtain

$$J_2 \simeq \int \frac{d^2\mathbf{k}_\perp}{2(2\pi)^3} \frac{g^4}{[m^2 + \mathbf{k}_\perp^2][m^2 + (\mathbf{k} - \mathbf{q})_\perp^2]} \int_{m^2/s}^1 \frac{d\beta}{m^2 + \mathbf{k}_\perp^2 - \beta s - i\varepsilon}. \tag{9.16}$$

It is the last denominator,

$$\frac{d\beta}{m^2 + \mathbf{k}_\perp^2 - \beta s - i\varepsilon} \simeq -\frac{1}{s} \frac{d\beta}{\beta},$$

that gives rise to the logarithm in the integration region (9.14):

$$J_2 \simeq -\frac{g^2}{s} \ln \frac{s}{m^2} \times \beta(q_\perp^2). \tag{9.17a}$$

Here we have introduced a convenient notation for the characteristic transverse momentum integral,

$$\beta(q_\perp) \equiv \int \frac{d^2\mathbf{k}_\perp}{2(2\pi)^3} \frac{g^2}{[m^2 + \mathbf{k}_\perp^2][m^2 + (\mathbf{k} - \mathbf{q})_\perp^2]}. \tag{9.17b}$$

The horizontal lines (3), (4) with large virtual momenta dropped out in the calculation of the asymptotic behaviour of the amplitude (9.6) and we have obtained a reduced diagram which contains only transverse momenta, and reminds of a Feynman diagram of a two-dimensional quantum field theory:

$$\begin{array}{c} p_1 \\ \swarrow \quad \searrow \\ \text{(3)} \\ \downarrow \quad \uparrow \\ k \quad k-q \\ \uparrow \quad \downarrow \\ \text{(4)} \\ \swarrow \quad \searrow \\ p_2 \end{array} \implies -\frac{g^2}{s} \ln \frac{s}{m^2} \times \begin{array}{c} g \\ \swarrow \quad \searrow \\ \text{loop} \\ \swarrow \quad \searrow \\ g \end{array} \tag{9.18}$$

Here comes a final refinement before we move to higher orders. The r.h.s. of (9.18) is real, while we know that the box diagram on the l.h.s. has an imaginary part when (and only when)  $s$  is positive. Can we find  $\text{Im } J_2$  without performing any calculations? It is actually very simple. Once we know  $\text{Re } J_2$ , in order to restore  $\text{Im } J_2$  it suffices to replace in (9.18)

$$\ln s \rightarrow \ln(-[s - i\epsilon]) = \ln s - i\pi. \tag{9.19}$$

This does not invalidate our asymptotic analysis since we have kept only the leading contribution  $\propto \ln s$  and systematically omitted all constant corrections,  $|i\pi| \ll \ln s$  being one of them. On the contrary, to keep this ‘special constant’ is legitimate, since it promotes our approximate expression to a true amplitude with proper analyticity.

It is time to guess the full answer. Let us try to add up the Born amplitude Fig. 9.1(b) and the next order correction (9.17) we have just derived:

$$\begin{array}{c} \text{tree} \\ + \\ \text{box} \\ + \dots \end{array} = -\frac{g^2}{s} - \frac{g^2}{s} \beta(q_\perp) \cdot \ln(-s) + \dots \tag{9.20}$$

$$\stackrel{?}{=} -\frac{g^2}{s} \cdot e^{\beta(q_\perp) \ln(-s)} = g^2(-s)^{-1+\beta(q_\perp)}.$$

If this guess is right, our two terms would be simply the first terms of the perturbative series expansion in  $\beta(q_\perp) = \mathcal{O}(g^2/m^2) \ll 1$  for the Regge pole amplitude.

9.2.4 Ladders in the leading logarithmic approximation

What will happen in higher orders? Take the third perturbative order,  $A \propto g^6$ , and imagine that we found a contribution  $A = \mathcal{O}(g^6 \ln s)$ . In spite of looking enhanced, this one is *insignificant* since when  $g^2 \ln s \sim 1$ , it constitutes but a small correction to the previous order,

$$A = A_{\text{Born}} \left( 1 + g^2 \ln s + \underline{g^2 \cdot g^2 \ln s} + \dots \right). \tag{9.21}$$

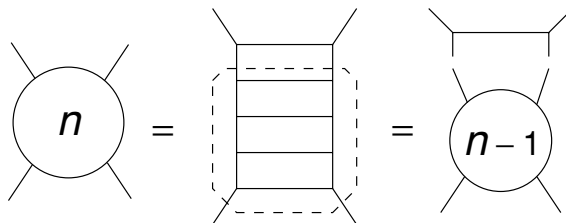
Now we have to look for  $A = \mathcal{O}(g^6 \ln^2 s)$ . In each order of the perturbation theory, with adding new internal momentum integration, we need to pick up an additional  $\ln s$  enhancement factor. In spite of an immense number of Feynman graphs in high orders, each can be analysed (and if necessary evaluated) approximately, in a search for  $(g^2 \ln s)^n$  terms. It is clear that not many diagrams will yield such a strong enhancement. Extracting and assembling such contributions in all orders constitutes the so-called ‘leading logarithmic approximation’,

$$A_{\text{LLA}} = A_{\text{Born}} \left( 1 + \sum_{n=1}^{\infty} f_n \cdot (g^2 \ln s)^n \right); \quad g^2 \ll 1, \quad g^2 \ln s \sim 1. \tag{9.22}$$

There is something important to stress. If we want the approximate amplitude  $A_{\text{LLA}}$  to represent the high-energy behaviour of the true scattering amplitude, the condition  $g^2 \ll 1$  is absolutely crucial. Only under this condition may we ignore a plethora of *subleading* corrections, like the one underlined in (9.21).

Let us draw the diagrams that do contribute in the LL approximation; we will check later that others do not. These are the  $n$ -particle ladders.

Note that a ladder with a given number of rungs can be constructed by adding the Born amplitude on top of the ladder of the previous order,



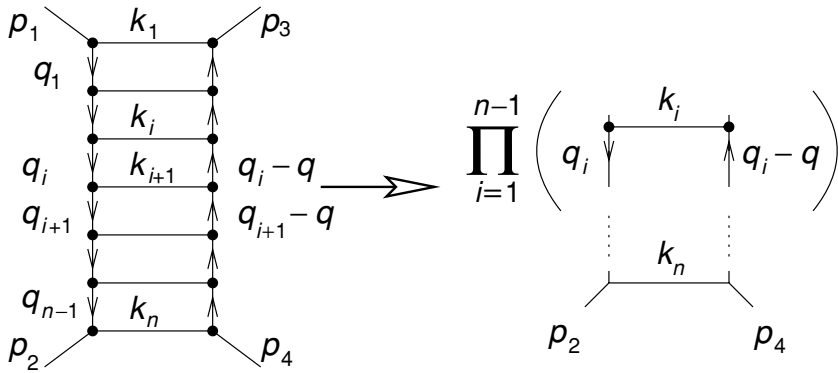


Fig. 9.4 Structure of the ladder diagram.

One can use this *t*-channel iterative nature of ladder graphs to derive the high energy behaviour of the amplitude  $A_{2\text{ton}\rightarrow 2}$  by induction. However, to gain a better understanding of the kinematics of ladder-type processes we shall proceed with a direct analysis of the structure of ladder amplitudes.

Consider an  $n$ -particle ladder shown in Fig. 9.4.

We have  $n - 1$  internal momentum integrals, and the amplitude  $J_n(s, q^2)$  can be written as

$$\begin{aligned}
 J_2 = & g^{2n} \prod_{i=1}^{n-1} \left( \int \frac{d^4 q_i}{(2\pi)^{4i}} \frac{1}{[m^2 - q_i^2][m^2 - (q_i - q)^2][m^2 - (q_{i-1} - q_i)^2]} \right) \\
 & \times \frac{1}{m^2 - (p_2 + q_{n-1})^2}, \tag{9.23}
 \end{aligned}$$

where in all propagators the Feynman shift is implied,  $m^2 \rightarrow m^2 - i\varepsilon$ . We have  $(n - 1)$  ‘blocks’, each containing two vertical,  $q_i$  and  $(q_i - q)$ , and one horizontal propagator,  $k_i = q_{i-1} - q_i$  ( $q_0 \equiv p_1$ ). The bottom rung,  $k_n = p_2 + q_{n-1}$ , closes the chain.

For the sake of convenience we will slightly modify the definition of the Sudakov variables as compared to (9.7) and write

$$\begin{aligned}
 q = \beta_q p'_1 - \alpha_q p'_2 + q_{\perp}, \quad \beta_q = \alpha_q = -\frac{q^2}{s} = \frac{\mathbf{q}_{\perp}^2}{s} \left( 1 + \mathcal{O}\left(\frac{m^2}{s}\right) \right); \tag{9.24} \\
 q_i = \beta_i p'_1 - \alpha_i p'_2 + q_{i\perp}, \quad q_i^2 = -\alpha_i \beta_i s - \mathbf{q}_{i\perp}^2.
 \end{aligned}$$

Thus  $\alpha_i$  and  $\beta_i$  enter in a more symmetric way: both positive, they describe the fraction of  $p_2$  transferred up the ladder and the fraction of  $p_1$  descending the ladder, respectively.

Have a look at the propagators of the horizontal lines, the ladder rungs:

$$k_1^2 = (p_1 - q_1)^2 = (\alpha_1 + \gamma)(1 - \beta_1)s + \dots, \tag{9.25a}$$

$$k_2^2 = (q_1 - q_2)^2 = (\alpha_2 - \alpha_1)(\beta_1 - \beta_2)s + \dots, \tag{9.25b}$$

$$k_i^2 = (q_{i-1} - q_i)^2 = (\alpha_i - \alpha_{i-1})(\beta_{i-1} - \beta_i)s + \dots, \tag{9.25c}$$

where we singled out the  $\alpha$  dependence. Suppose now that we evaluate the  $\alpha_i$  integrals by putting the rungs, one by one, on the mass shell as we did before in the  $n = 2$  case when we closed the contour around the pole (3), see (9.13). The residue in  $\alpha_1$  equals  $1/(1 - \beta_1)s$ ; then  $\alpha_2$  gives  $1/(\beta_1 - \beta_2)s$ , etc. The bottom rung will produce one more factor,

$$m^2 - k_n^2 = m^2 - (q_{n-1} + p_2)^2 = m^2 + \mathbf{k}_{n\perp}^2 - (1 - \alpha_{n-1})(\beta_{n-1} + \gamma)s, \tag{9.25d}$$

in the denominator. Combining all  $\beta$ -dependent factors, the following structure of the  $\beta_i$  integrals emerges:

$$J_n \sim \frac{1}{1 - \beta_1} \frac{d\beta_1}{\beta_1 - \beta_2} \frac{d\beta_2}{\beta_2 - \beta_3} \dots \frac{d\beta_{n-2}}{\beta_{n-2} - \beta_{n-1}} \frac{d\beta_{n-1}}{\beta_{n-1} + \gamma}. \tag{9.26}$$

How can we get many logarithms? We need to gain one logarithm per *each* integration. One can easily prove that it is necessary to arrange successive  $\beta_i$ s as follows:

$$1 \gg \beta_1 \gg \beta_2 \gg \dots \gg \beta_i \gg \dots \gg \beta_{n-1} \gg \gamma = \frac{m^2}{s}. \tag{9.27a}$$

What about the  $\alpha$ s? They, too, turn out to be strongly ordered. Indeed, applying (9.27a) to (9.25) leads to the following pattern:

$$\alpha_1 \sim \frac{m_{1\perp}^2}{s}, \quad \alpha_2 \sim \frac{m_{1\perp}^2}{\beta_1 s}, \quad \dots \quad \alpha_i \sim \frac{m_{i\perp}^2}{\beta_{i-1} s}, \quad \dots \quad \alpha_{n-1} \sim \frac{m_{n-1,\perp}^2}{\beta_{n-2} s},$$

where  $m_{i\perp}^2 \equiv m^2 + \mathbf{k}_{i\perp}^2 = \mathcal{O}(m^2)$ . Combining with (9.27a), we get

$$\frac{m_{1\perp}^2}{s} \sim \alpha_1 \ll \alpha_2 \ll \dots \ll \alpha_i \ll \dots \ll \alpha_{n-1} \ll 1; \tag{9.27b}$$

$$\alpha_i \beta_{i-1} s \sim m_{i\perp}^2, \quad i = 1, \dots, n - 1 \quad (\beta_0 \equiv 1). \tag{9.27c}$$

Inequalities (9.27) show that the flows of  $p_1$  and  $p_2$  momenta along the ladder are opposite and strongly ordered: ascending the ladder, the fractions of  $p_2$  ( $\alpha_i$ ) successively *decrease*, in accord with the strong *increase* of  $\beta_i$  (fraction of  $p_1$ ).

Given the strong ordering of  $\beta$ s, (9.26) reduces to

$$J_n \sim \int^1 \frac{d\beta_1}{\beta_1} \int^{\beta_1} \frac{d\beta_2}{\beta_2} \cdots \int^{\beta_{n-3}} \frac{d\beta_{n-2}}{\beta_{n-2}} \int_{\gamma}^{\beta_{n-2}} \frac{d\beta_{n-1}}{\beta_{n-1}},$$

giving

$$J_n \sim \frac{1}{(n-1)!} \left( \int_{\gamma}^1 \frac{d\beta}{\beta} \right)^{n-1}.$$

Now we can complete the calculation of  $J_n$ . Due to the estimate (9.27c), a crucial simplification emerges: the longitudinal variables drop out from all *vertical lines*. Indeed,

$$m^2 - q_i^2 = m^2 + \mathbf{q}_{i\perp}^2 + \alpha_i \beta_i s = m_{i\perp}^2 + \alpha_i \beta_{i-1} s \cdot \frac{\beta_i}{\beta_{i-1}} \simeq m_{i\perp}^2,$$

where we have used (9.27c) and the strong  $\beta$ -ordering,  $\beta_i/\beta_{i-1} \ll 1$ . Thus in the logarithmic region (9.27) the dependences on  $\mathbf{q}_{i\perp}$  and  $\beta_i$  fully separate and leave us with  $n-1$  identical transverse momentum loop integrals (9.17b) resulting in

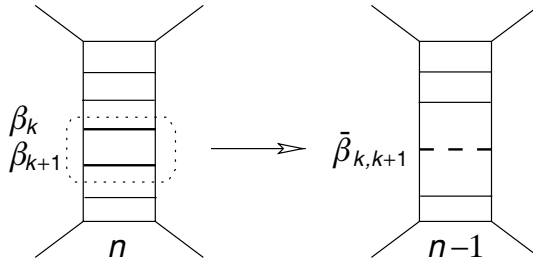
$$J_n = -\frac{g^2}{s} \frac{1}{(n-1)!} \ln^{n-1} \left( \frac{-s}{m^2} \right) \cdot [\beta(q_{\perp})]^{n-1}. \quad (9.28)$$

We changed the sign of  $s$  under the logarithm to restore analyticity of the amplitude properly, as we have discussed before, when we analysed  $J_2$ . Summing over  $n$  we obtain the Regge-like expression (9.20) that we have guessed above.

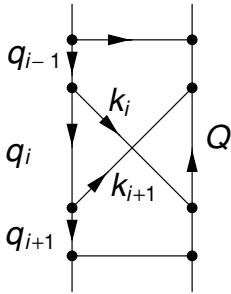
Before discussing the final result, let us verify that the ladder diagrams in the kinematical region (9.27) are indeed the only ones to contribute.

First of all, it is clear from (9.26) that a decision to *swap*  $\beta$ s in the ordering condition (9.27a) immediately results in a loss of (at least) one logarithmic factor. To have  $\beta$ s *strongly* ordered is also essential. If we keep two neighbouring momenta of the same order,  $\beta_k \sim \beta_{k+1}$ , such a pair can be treated as a single rung with the effective ‘mean’ momentum  $\bar{\beta} = \sqrt{\beta_k \beta_{k+1}}$ , effectively reducing the ladder  $J_n$  to  $J_{n-1}$  and thus losing one  $\ln s$ ,

$$\iint \frac{d\beta_k d\beta_{k+1}}{\beta_k \beta_{k+1}} = \int \frac{d\bar{\beta}}{\bar{\beta}} \cdot \int d \ln \left( \frac{\beta_k}{\beta_{k+1}} \right) \implies \ln s \cdot \mathcal{O}(1).$$



The same thing happens if we allow any rungs to cross.



The momentum  $Q$ , which used to be  $Q = q_i - q$  in the plain ladder, becomes in the crossed configuration

$$Q = [q_{i+1} + q_{i-1} - q_i] - q. \tag{9.29}$$

It inherits the largest  $\alpha$ -component from  $q_{i+1}$ , and the  $\beta$ -component from  $q_{i-1}$ , so that the new virtual denominator becomes

$$m^2 - Q^2 \simeq \alpha_{i+1}\beta_{i-1}s + m^2 + Q_{\perp}^2.$$

Invoking (9.27c) we see that the ‘longitudinal’ part of the virtuality is no longer negligible; on the contrary, the new denominator is very large,

$$m^2 - Q^2 \sim m_{\perp}^2 \cdot \frac{\beta_{i-1}}{\beta_i} \gg m_{Q\perp}^2;$$

its presence spoils the logarithmic integration over  $\beta_i$ ,

$$\int \frac{d\beta_{i-1}}{\beta_{i-1}} \int^{\beta_{i-1}} \frac{d\beta_i}{\beta_i} \cdot \left(\frac{\beta_{i-1}}{\beta_i}\right)^{-1} \sim \int \frac{d\beta_{i-1}}{\beta_{i-1}} \times 1,$$

and we have  $\beta_{i+1} \sim \beta_i$ , i.e. the situation that we have just discussed. The appearance of a large virtuality has a transparent physical explanation. Momenta of the ladder rungs,  $k_i$ , are very different in scale. For example, in the rest frame of  $p_2$  we have

$$k_i \simeq (\beta_{i-1} - \beta_i)p_1 \approx \beta_{i-1}p_1, \quad k_{i+1} \simeq (\beta_i - \beta_{i+1})p_1 \approx \beta_i p_1,$$

so that the successive particle is much *softer* than its predecessor,

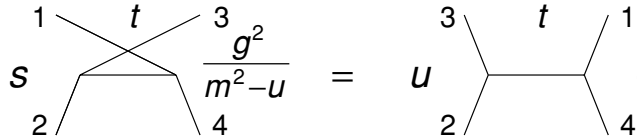
$$\frac{k_{i+1}}{k_i} \simeq \frac{\beta_i}{\beta_{i-1}} \ll 1.$$

This is favourable for the *production* of particles  $k_i, k_{i+1}$  (the left side of the graph). However, on the *absorption* side (the right half of the graph), the natural ordering is just opposite. In the lower vertex a hard particle

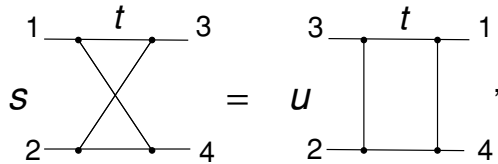
has to be absorbed where there used to be a soft one, causing a large recoil.

9.2.5 Reggeon as a sum of ladder graphs

Up to now we were dealing with the high-order amplitudes that one obtains iterating in the  $t$ -channel the ‘ $s$ -channel’ Born graph Fig. 9.1b. Exactly the same considerations can be carried out for the ‘ $u$ -channel’ amplitude (9.1c), which differs from the graph that we have iterated by the crossing transformation  $s \leftrightarrow u$ .



Under the crossing the second-order amplitude of Fig. 9.2 turns into the familiar box,



etc. Thus, in order to obtain the second series of contributions, we simply have to substitute  $s \rightarrow u \simeq -s$  in our answer (9.28).

The final answer for the high-energy behaviour of the amplitude reads

$$A(s, t) \simeq \sum_{n=1}^{\infty} J_n = \frac{g^2}{m^2} \left[ \left( \frac{-s}{m^2} \right)^{-1+\beta(t)} + \left( \frac{s}{m^2} \right)^{-1+\beta(t)} \right], \quad (9.30a)$$

$$\beta(t) = \int \frac{d^2 \mathbf{k}_{\perp}}{2(2\pi)^3} \frac{g^2}{[m^2 + \mathbf{k}_{\perp}^2][m^2 + (\mathbf{k} - \mathbf{q})_{\perp}^2]}; \quad t \simeq -\mathbf{q}_{\perp}^2. \quad (9.30b)$$

Strictly speaking, we cannot claim that (9.30) describes the true *asymptotics*  $s \rightarrow \infty$ , since our leading logarithmic approximation (9.22) applies to very large but finite energies,

$$s \lesssim m^2 \exp \left\{ \frac{m^2}{g^2} \right\}.$$

Nevertheless, let us compare our result (9.30a) with the Regge pole amplitude,

$$A_{\text{pole}}^{\pm}(s, t) = -\frac{r(t)}{\sin \pi \alpha(t)} \left[ \left( \frac{-s}{m^2} \right)^{\alpha(t)} \pm \left( \frac{s}{m^2} \right)^{\alpha(t)} \right].$$





Indeed, let us calculate the partial wave corresponding to the  $s$ -channel exchange amplitude. Substituting

$$A_1(s, t) = \text{Im} \left\langle \frac{g^2}{m^2 - s - i\epsilon} \right\rangle = g^2 \cdot \pi \delta(m^2 - s)$$

in the general expression (7.27b),

$$\begin{aligned} f_\ell(t) &= \frac{2}{\pi} \int_{z_0}^{\infty} dz_s A_1(t, s) Q_\ell(z_s) \\ &= \frac{4}{\pi(t - 4m^2)} \int_{s_0}^{\infty} ds A_1(t, s) Q_\ell \left( 1 + \frac{2s}{t - 4m^2} \right), \end{aligned}$$

we obtain

$$f_\ell(t) = \frac{4g^2}{t - 4m^2} Q_\ell \left( 1 + \frac{2m^2}{t - 4m^2} \right) \stackrel{\ell \rightarrow -1}{\sim} \frac{4g^2}{t - 4m^2} \cdot \frac{1}{\ell + 1}. \quad (9.32a)$$

Comparing with the partial wave of the amplitude (9.30a),

$$f_\ell(t) \sim \frac{1}{\ell + 1 - \beta(t)}, \quad (9.32b)$$

we conclude that since  $\beta(t) \ll 1$ , generically our reggeon is connected to the fixed pole (9.32a) at  $\ell = -1$ .

One has to remember that the results of this section are valid only for  $g^2/m^2 \ll 1$ . The Regge trajectory which we got under this condition,

$$\alpha = -1 + \beta(t),$$

has no relation to the observed trajectories with hadron resonances placed on them. Nevertheless, the example of the  $g\varphi^3$  theory is rather instructive, as it demonstrates what kind of  $s$ -channel processes may correspond to real Regge poles. But before turning to the  $s$ -channel structure of the reggeon exchange, let us briefly discuss what happens in other theories.

### 9.2.6 Reggeization in other theories

Thus, the scalar meson representing the  $\phi$  field of the  $g\phi^3$  quantum field theory remained an elementary particle. At the same time, a Regge trajectory appeared that corresponds in fact to a two-particle bound state (sort of ‘positronium’).

As for other theories, there are not many since we can operate only with renormalizable ones.

*Fermion + scalar.* If we take a renormalizable field theory based on spin  $\frac{1}{2}$  fermions interacting with a scalar field,  $\mathcal{L}_{\text{int}} \sim \bar{\psi}\psi\phi$ , the answer is similar: the input objects stay elementary, while their bound states do reggeize.

*Fermion + vector.* A field theory of the type of quantum electrodynamics provides a more telling example. Once again, we take spin- $\frac{1}{2}$  ‘electrons’ and couple them to a vector field,

$$\begin{array}{ccc} \sigma=\frac{1}{2} & \sigma=1 & \\ \hline m & \mu & \text{---} \diagup \text{---} \\ & & \text{---} \diagdown \text{---} \end{array} = \gamma_\mu.$$

In this theory a curious thing happens. Look at the Compton process in the region of fixed  $u$  (backward scattering). Summing up perturbative radiative corrections in the approximation  $e^2 \ll 1$ ,  $e^2 \ln s \sim 1$  (LLA),

$$\begin{array}{c} \text{---} \text{---} \\ | \\ \text{---} \text{---} \end{array} + \begin{array}{c} \text{---} \text{---} \\ | \diagup \\ \text{---} \text{---} \end{array} + \begin{array}{c} \text{---} \text{---} \\ | \text{---} \\ \text{---} \text{---} \end{array} + \dots = r\xi_\alpha S^\alpha \quad (9.33)$$

$\alpha(u) \ln s \qquad \alpha^2(u) \ln^2 s$

a reggeon emerges. What is even better, its trajectory satisfies the relation  $\alpha(m_e^2) = \frac{1}{2}$ . A remarkable phenomenon: in QED with a massive photon, the fermion *reggeizes*! How did it occur? In the Born approximation we have a fixed pole in the partial wave,

$$f_j^{\text{Born}} \propto \frac{e^2}{m^2 - u} \delta_{j, \frac{1}{2}}. \quad (9.34)$$

Analogously to the scalar case, see (9.31b), the reggeon residue  $r$  in (9.33) is of the second order in the squared coupling,  $r = \mathcal{O}(e^4)$ . How can the first-order expression (9.34) be a part of it? What happens in higher orders is that (9.34) becomes a *limiting value* of the function

$$f_j = \text{const} \frac{e^4}{j - \frac{1}{2} - \beta(u)}, \quad \beta \propto e^2, \quad \beta(m^2) = 0. \quad (9.35)$$

For angular momenta  $j \neq \frac{1}{2}$ , the specific contribution (9.35) to the partial wave is  $\mathcal{O}(e^4)$  and can be neglected. At the same time, if we take the

angular momentum (very close to)  $j = \frac{1}{2}$ ,

$$f_{j \rightarrow \frac{1}{2}} = \text{const} \frac{e^4}{-\beta(u)} = \frac{e^2}{m^2 - u},$$

the magnitude of the partial wave becomes normal, and reproduces the Born amplitude (9.34).

In the usual electrodynamics where the photon is massless,  $\mu = 0$ , a complication emerges due to the standard infrared divergence.

In the  $\mu \rightarrow 0$  limit, the one-particle pole collides with thresholds due to additional photons:  $m + n \cdot \mu \rightarrow m$ . As a result, the electron Green function at  $p^2 = m^2$  does not have a pole anymore but develops a more tricky singularity. Nevertheless, in QED one can also claim that the electron lies on the Regge trajectory in the following sense. Whatever the nature of the singularity, the *position* of this whole thing *reggeizes*, that is moves with  $j$ ,  $m_e^2 \rightarrow m^2(j)$ .

Formally speaking,  $\alpha(t)$  describing the elastic  $e\gamma$  scattering amplitude (9.33) diverges in the infrared region and becomes undefined. This is natural: purely elastic processes do not exist in QED; taking into account the infrared radiative corrections, elastic amplitudes vanish. However, if one considers observables that are insensitive to the emission of undetectable, infinitely soft photons, the physical cross sections become finite, and the electron trajectory can be properly defined,

$$\frac{d\sigma}{d\Omega} \propto s^{2(\alpha(u)-1)}, \quad \alpha(m_e^2) = \frac{1}{2}. \quad (9.36)$$

A QED photon does not reggeize.

*Yang–Mills fields.* Recently\* a new class of very interesting renormalizable field theories was found, the Yang–Mills theories. The scheme includes self-interacting massless vector fields and fermions, as well as some additional scalars ('ghost'). In this theory both fermions and vector particles reggeize.

### 9.2.7 Non-pole singularities in perturbation theory

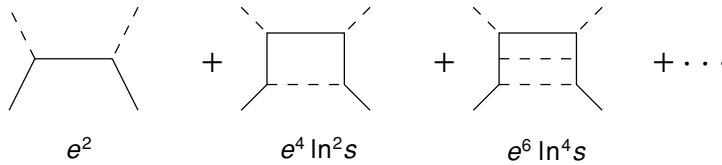
We have a couple of questions more to ask to the perturbation theory:

- (1) are there singularities other than poles?
- (2) any hints about the pomeron that we need for  $\sigma_{\text{tot}} \rightarrow \text{const}$ ?

---

\* The lecture was in 1975 (ed.)

The  $g\phi^3$  field theory contains nothing but Regge poles. In all other theories, however, there are non-pole singularities too. Take QED as an example and consider once again the Compton scattering, but this time in the *forward* kinematics,  $|t| \sim m^2 \ll s \simeq -u$ . Interesting contributions will be the following:



The analysis of the ladder diagrams of this type follows the steps of the scalar case, and in the leading approximation one arrives at the exponential of the reduced two-dimensional diagram describing the trajectory,

$$\begin{array}{c} e \\ \diagup \quad \diagdown \\ \bullet \\ \diagdown \quad \diagup \\ k \quad \quad k-q \\ \diagup \quad \diagdown \\ \bullet \\ \diagdown \quad \diagup \\ e \end{array} = \frac{e^2}{4\pi} \int \frac{d^2\mathbf{k}_\perp}{(2\pi)^2} \frac{1}{[m - \hat{k}][m - (\hat{q} - \hat{k})]}. \tag{9.37}$$

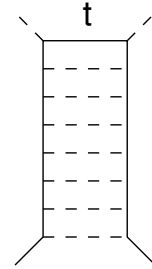
Contrary to the scalar loop, this integral *diverges* in the large momentum region! What does this mean? Our initial diagrams were convergent in the ultraviolet. So this must be not a real divergence but an artefact of the approximations made.

Indeed, we carried out the analysis of the ladder kinematics, estimated the virtualities etc. having *supposed* that transverse momenta are limited,  $\mathbf{k}_\perp^2 \ll s$ . In the scalar theory this working hypothesis found its confirmation in the end of the calculation: the integral for  $\beta(q_\perp)$  converged at  $\mathbf{k}_\perp^2 \sim m^2$ . In QED, in a contrast to the super-convergent  $g\phi^3$  theory, the coupling constant is dimensionless, and the  $k_\perp$  integration produces another logarithm,

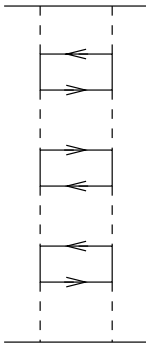
$$\begin{array}{c} e \\ \diagup \quad \diagdown \\ \bullet \\ \diagdown \quad \diagup \\ k \quad \quad k-q \\ \diagup \quad \diagdown \\ \bullet \\ \diagdown \quad \diagup \\ e \end{array} \sim e^2 \int_{m^2}^s \frac{d\mathbf{k}_\perp^2}{\mathbf{k}_\perp^2} = e^2 \ln \frac{s}{m^2}. \tag{9.38}$$

So, in the second order, e.g. the ‘box’ diagram acquires two logs,  $e^4 \ln^2 s$ , instead of one,  $e^4 \ln s$ . Such a series corresponds in the angular momentum plane not to a Regge pole but to a different singularity.

From the  $t$ -channel point of view this problem resembles a non-relativistic system with a singular potential. You may remember that we have discussed how in non-relativistic quantum mechanics an interaction singular at small distances gave rise to fixed poles. We considered a non-relativistic potential  $V \propto -c/r^2$  which corresponds to the ‘falling on the centre’ phenomenon. We noted that if the parameter  $c$  is not too large,  $c < \frac{1}{4}$ , then physically there is no catastrophic ‘falling on the centre’, but a fixed pole in the partial wave appears near zero,  $j_0 = ce^2$ . This is what happens in the *forward* Compton scattering problem.



Another interesting question: is there not a singularity at  $j=1$  in QED? Look at the Feynman graphs with many electron loops inserted in the two photon exchange diagram.



Cutting through such diagrams one gets the total cross section *increasing* with energy,

$$\text{Im } A \sim e^4 s^{1+\gamma}, \quad \gamma \sim e^4; \quad \sigma \propto s^\gamma. \quad (9.39)$$

Such a behaviour corresponds to a fixed singularity at  $j_0 > 1$ . This high-energy behaviour is valid as long as  $e^4 \ln s \lesssim 1$ . At yet higher energies the power increase (9.39) must stop, according to the Froissart theorem, and the true position of the singularity should move to the left. A theoretical analysis of how this happens is lacking.

Theoretical studies of the high-energy behaviour of various QED processes left a number of unanswered questions. At the same time, they provided a certain experience which allows one to make conclusions about what can happen *beyond* the perturbation theory.

### 9.3 Inelastic processes at high energies

We embark on a discussion of a very important issue, namely what inelastic processes a Regge pole corresponds to.

We have seen that in the  $g\varphi^3$  theory the Regge pole appears as a sum of multi-particle ladders:

$$A(s, t) = \sum \text{[Ladder Diagrams]} = \text{[Wavy Line Diagram]} = \frac{g^2}{m^2} \left[ \left( \frac{-s}{m^2} \right)^{-1+\beta(t)} + \left( \frac{s}{m^2} \right)^{-1+\beta(t)} \right].$$

Evaluating the imaginary part of the forward elastic amplitude we obtain, due to the optical theorem, the total cross section:

$$\sigma_{\text{tot}} \simeq s^{-1} \text{Im } A(s, 0) \simeq \frac{g^2}{s^2} \left[ \pi\beta(0) \left( \frac{s}{m^2} \right)^{\beta(0)} \right], \tag{9.40a}$$

where we invoked (9.19) to fix the phase of the complex factor  $(-s)^\beta$  and expanded perturbatively  $\sin \pi(1 - \beta) \simeq \pi\beta$ . Since  $\beta(0) > 0$ , the total cross section (9.40a) decreases slower with  $s$  and is therefore *much larger* at high energies than the Born elastic cross section,

$$\sigma_{\text{Born}}^{\text{el}} \propto \int \frac{d\Omega}{4\pi} \left| \frac{A(s, t)}{s} \right|^2 \sim \frac{g^4}{s^2}. \tag{9.40b}$$

This means that inelastic channels dominate.

### 9.3.1 Topological cross sections $2 \rightarrow 2 + n$

Having our ladder pictures, it is straightforward to find not only total but all partial inelastic cross sections as well. Indeed, since  $\sigma_{\text{tot}}$  is determined by the sum

$$\text{Im } A(s, 0) = \sum_{k=2} \text{Im } J_k(s, 0),$$

where  $J_k$  is one of the ladder graphs, we have

$$\begin{aligned} \sigma_{n+2} &= s^{-1} \text{Im } J_{n+2}(s, 0) = -\frac{g^2}{s} \text{Im} \frac{[\beta(0)(\ln s - i\pi)]^{n+1}}{(n+1)!} \\ &\simeq \frac{\pi g^2 [\beta(0)]^{n+1}}{s^2 n!} \ln^n s \sim \sigma_{\text{Born}}^{\text{el}} \cdot \frac{[\beta(0) \ln s]^n}{n!}; \end{aligned} \tag{9.41}$$

here  $\sigma_{n+2}$  (the so-called ‘topological cross sections’) is the cross section of the process  $2 \rightarrow 2 + n$  with the production of  $n$  additional particles. What is the characteristic number of produced particles in the sub-processes that have made  $\sigma_{\text{tot}}$  increase with respect to the elastic one? The expression (9.41) is nothing but a *Poisson distribution* in multiplicity

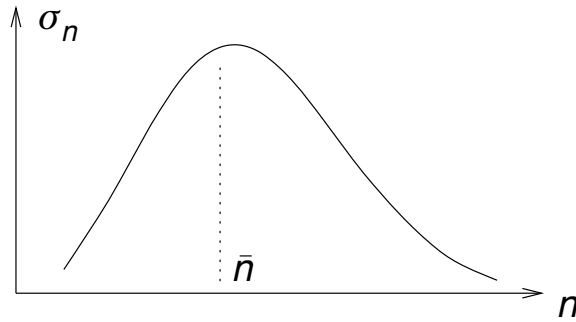


Fig. 9.5 Poisson multiplicity distribution of topological cross sections.

which we can represent invoking (9.40) as

$$\frac{\sigma_{n+2}}{\sigma_{\text{tot}}} = \frac{\bar{n}^n}{n!} e^{-\bar{n}}, \quad \sigma_{\text{tot}} = \sum_{n=0}^{\infty} \sigma_{n+2}. \tag{9.42a}$$

Here  $\bar{n}(s)$  is the logarithmically increasing average particle multiplicity,

$$\bar{n} = \bar{n}(s) \simeq \beta(0) \ln \frac{s}{m^2}. \tag{9.42b}$$

So it is inelastic sub-processes with the number of particles increasing with energy,  $n \sim \bar{n}$ , that dominate the total cross section as shown in Fig. 9.5.

### 9.3.2 Multiperipheral kinematics

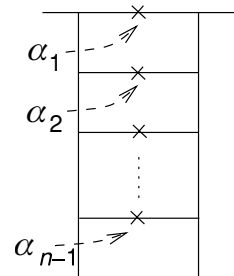
Another interesting question is how the produced particles are distributed. To answer it, we need to look into the internal structure of the ladders. Recall how we calculated above the ladder diagram  $J_n$ .

We have introduced  $n - 1$  momenta of the vertical lines,  $q_i$ , and took the residues in  $\alpha_i$  putting on the mass shell all the rungs but the very bottom one. This last particle also becomes real when we take the imaginary part of  $J_n$ , see (9.25d),

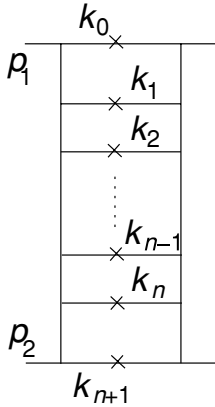
$$\int d\beta_{n-1} \text{Im} \frac{1}{m_{n\perp}^2 - i\varepsilon - (1 - \alpha_{n-1})(\beta_{n-1} + \gamma)s} = \frac{\pi}{s},$$

fixing the value of  $\beta_{n-1}$ .

Since we are interested in the distribution of the produced particles, it is natural to express the ladder in terms of the final-state momenta,  $k_i$ .







Let us take  $J_{n+2}$ . The top and bottom particles are ‘leaders’: the top one has a large  $\beta$ -component,

$$\beta_0^{(k)} = 1 - \beta_1 \simeq 1, \quad k_0 \simeq p_1 + \frac{m_{0\perp}^2}{s} p_2 + k_{0\perp},$$

and the bottom particle, correspondingly, carries away practically all the momentum of  $p_2$ ,

$$\beta_{n+1}^{(k)} \simeq \frac{m_{n+1,\perp}^2}{s}, \quad k_{n+1} \simeq p_2 + \frac{m_{n+1,\perp}^2}{s} p_1 + k_{n+1,\perp}.$$

At the same time, the longitudinal momenta of all ‘new’ particles,  $i = 1, 2, \dots, n$ , change freely, and it is these variations that enhance the cross section. Translating  $q_i$  into the rung momenta  $k_i = q_i - q_{i+1}$ , see (9.27),

$$\beta_i^{(k)} = \beta_i - \beta_{i+1} \simeq \beta_i, \tag{9.43a}$$

$$\alpha_i^{(k)} = \alpha_{i+1} - \alpha_i \simeq \alpha_{i+1}; \tag{9.43b}$$

for  $J_{n+2}$  we have

$$\text{Im } J_{n+2} = \frac{\pi g^2}{s} \prod_{i=1}^{n+1} \left\{ \int \frac{d^2 \mathbf{k}_{i\perp}}{2(2\pi)^3} \frac{g^2}{(i_\perp)^2} \right\} \int^1 \frac{d\beta_1}{\beta_1} \dots \int_\gamma^{\beta_{n-1}} \frac{d\beta_n}{\beta_n}. \tag{9.44}$$

Evaluating the integrals results in the multiplicity distribution (9.41). The integrand itself gives us the momentum spectra of final-state particles in the process  $2 \rightarrow 2 + n$ . We observe two important properties.

- (1) Dependences on transverse and longitudinal variables of final-state particles,  $k_{i\perp}$  and  $k_{iz} \propto \beta_i$ , factorized.
- (2) The distribution is *uniform* in

$$\frac{d\beta_i}{\beta_i} = d(\ln \beta_i). \tag{9.45}$$

Such a pattern of multi-particle production (not to forget the limited transverse momenta) is often referred to as ‘multiperipheral kinematics’.

In the laboratory frame, with the target at rest,  $\mathbf{p}_2 = 0$ , and the projectile very fast,  $p_{10} \simeq s/2m$ ,  $k_i \simeq \beta_i p_1$ , so that one may speak of the uniformity in  $\ln k_{i0}$ . This means that, descending the ladder, we will typically meet particles with energies

$$k_{10} \sim \lambda \cdot p_{10}, \quad k_{20} \sim \lambda^2 \cdot p_{10}, \quad \dots, \quad k_{n0} \sim \lambda^n \cdot p_{10}, \tag{9.46}$$

all the way down to the target,  $k_{n+1,0} \sim \lambda^{n+1} \cdot p_{10} = m$ . The energy fraction  $\lambda$  is a measure of the invariant mass squared of the neighbouring particles:

$$\begin{aligned}
 s_{12} &= (k_1 + k_2)^2 \sim 2(k_1 k_2) = (\beta_1 \alpha_2 + \beta_2 \alpha_1) s \\
 &= \beta_1 \frac{m_{2\perp}^2}{\beta_2} + \beta_2 \frac{m_{1\perp}^2}{\beta_1} \sim (\lambda^{-1} + \lambda) m_{\perp}^2 \simeq \frac{m_{\perp}^2}{\lambda},
 \end{aligned}
 \tag{9.47}$$

where we substituted  $\alpha_1, \alpha_2$  from the on-mass-shell conditions,

$$\alpha_i \beta_i s = m^2 + \mathbf{k}_{i\perp}^2 \equiv m_{i\perp}^2.
 \tag{9.48}$$

We have

$$(n + 1) \cdot \ln \lambda^{-1} \simeq \ln \frac{P}{m} \simeq \ln \frac{s}{m^2};$$

substituting the average multiplicity (9.42b), we get an estimate

$$\ln \lambda^{-1} \simeq \ln \frac{\langle s_{i,i+1} \rangle}{\langle m_{i\perp}^2 \rangle} \simeq \frac{1}{\beta(0)} \propto \frac{1}{\bar{g}^2} \quad \left( \bar{g}^2 \equiv \frac{g^2}{m^2} \right),
 \tag{9.49}$$

with  $\bar{g}$  the dimensionless coupling constant. We see that the pair masses of the neighbours are very large in the perturbation theory where the coupling constant is small. It is worthwhile to mention here a kinematical relation linked to this observation. Let us construct the product of all pair invariants along the multiperipheral chain:

$$s_{01} s_{12} s_{23} \cdots s_{n-1,n} s_{n,n+1}.$$

Using  $s_{i,i+1} \simeq \beta_i \alpha_{i+1} s$  (cf. (9.47)),

$$(\beta_0 \alpha_1 s) (\beta_1 \alpha_2 s) \cdots (\beta_{n-1} \alpha_n s) (\beta_n \alpha_{n+1} s),$$

and assembling the products (9.48), we get

$$\prod_{i=0}^n s_{i,i+1} = \beta_0 \cdot \prod_{i=1}^n (\alpha_i \beta_i s) \cdot \alpha_{n+1} s = s \cdot \prod_{i=1}^n m_{i\perp}^2,
 \tag{9.50}$$

where we have used  $\beta_0 \simeq \alpha_{n+1} \simeq 1$  for the leading particles. The substitution of the average characteristics gives

$$\langle s_{i,i+1} \rangle^{\bar{n}} = \langle s \rangle^{\beta(0) \ln s} = s^{\beta(0) \ln \langle s \rangle} = s, \implies \beta(0) \ln \langle s \rangle = 1,$$

reproducing (9.49).

9.3.3 Inclusive particle spectrum

What sort of observables should we measure in the case of a large multiplicity? It is interesting to study the average characteristics of particle production, for example, to plot a histogram for the longitudinal momentum distribution. Let us introduce an important observable which is well suited for characterizing multi-particle production. Consider the density of particles per unit cell of the momentum phase space,

$$d^3\sigma^{\text{incl}}(\mathbf{k}) = f(k) \frac{d^3\mathbf{k}}{k_0}.$$

To measure this quantity, one has to register *one particle* with a given momentum  $\mathbf{k}$  and ignore the number, and momenta, of other particles produced in the collision. Take for an example a  $pp$  collision and trigger one meson.

$$\sum_n \left| \begin{array}{c} \text{Diagram: A circle representing a collision vertex. Two incoming lines from the left are labeled } p. \text{ One outgoing line to the top right is labeled } k \text{ and } \pi^-. \text{ Multiple outgoing lines to the right are labeled } k_1, \dots, k_{n-1}. \end{array} \right|^2 d\Gamma_{n-1} = d\sigma(k).$$

We square the  $n$ -particle production amplitude  $A$ , integrate indiscriminately over the momenta of all final-state particles but one  $\pi^-$  with momentum  $\mathbf{k}$  and sum over all ‘topologies’  $n$ . This quantity is called the ‘inclusive spectrum’, in contrast to ‘exclusive’ processes (like elastic scattering) where characteristics of all final-state particles are measured.

One should be aware of the fact that  $f$  is *not* a differential cross section in a sense, because its integral does not yield  $\sigma_{\text{tot}}$ . Write down the general expression for the inclusive one-particle spectrum,

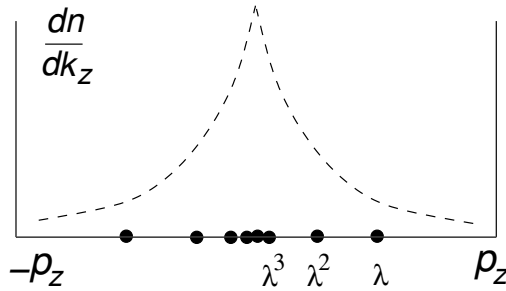
$$d^3\sigma = \frac{1}{j} \sum_n \frac{d^3k}{2(2\pi)^3 k_0} \cdot \frac{1}{(n-1)!} \int \dots \int \frac{d^3k_1 \dots d^3k_{n-1}}{(2\pi)^{3(n-1)} 2k_{10} \dots 2k_{n-1,0}} \quad (9.51)$$

$$\times |A_n(k; k_1, \dots, k_{n-1})|^2 (2\pi)^4 \delta(p_1 + p_2 - k - \sum k_i).$$

Essential here is the combinatorial factor  $1/(n-1)!$  which takes care of multiple counting in the integration over the full phase space of  $n-1$  identical particles. If we wanted to calculate  $\sigma_{\text{tot}}$ , we would have to integrate over all particle momenta, including  $k$ , with the factor  $1/n!$ . Therefore, integrating (9.51) over the momentum of the selected particle we will obtain not the total cross section  $\sigma_{\text{tot}} = \sum_n \sigma_n$ , but  $\sum_n n\sigma_n \equiv \bar{n}\sigma_{\text{tot}}$ , with  $\bar{n}$  the average multiplicity.

9.3.4 Rapidity variable

How to examine inclusive cross sections? It makes little sense to plot it in the bins in  $k_z$  since, because of the strong ordering (9.27), (9.46), the bulk of particles is *soft*,  $|k_z| \ll p_z$ , and will fall into the single bin around  $k_z \simeq 0$ , in any reference frame. For example, in the cms we will not see anything but a huge peak in the centre of the distribution,



Uniformity of multiperipheral particle production in  $d\beta/\beta$  means constant particle density per unit of phase space,

$$d\Gamma(k) = \frac{d^3\mathbf{k}}{k_0} = d^2\mathbf{k}_\perp \frac{dk_z}{k_0}, \quad \frac{dk_z}{k_0} = \frac{d\beta}{\beta}.$$

To characterize this key feature of multi-particle production in a Lorentz-covariant manner, one introduces a convenient variable called ‘rapidity’,

$$\eta = \frac{1}{2} \ln \frac{k_0 + k_z}{k_0 - k_z}. \tag{9.52a}$$

Using the on-mass-shell relation  $(k_\mu)^2 = m^2$ , we may rewrite (9.52a) as

$$\eta = \frac{1}{2} \ln \frac{(k_0 + k_z)^2}{k_0^2 - k_z^2} = \ln \frac{k_0 + k_z}{m_\perp}. \tag{9.52b}$$

In the frame where  $k$  is fast,  $|\eta| \simeq \ln(2k_0/m_\perp)$  (the sign being that of  $k_z$ ). This variable is special in the sense that it transforms *additively* under Lorentz boosts along the collision axis  $\mathbf{z}$ ,

$$\eta \rightarrow \eta + \Delta\eta, \quad \Delta\eta = \frac{1}{2} \ln \frac{1+v}{1-v}.$$

The *relative* rapidity of two particles is therefore invariant under such a change of the reference frame. Observing that the energy and the longitudinal momentum can be expressed in terms of the rapidity (9.52) as

$$k_0 = m_\perp \cosh \eta, \quad k_z = m_\perp \sinh \eta,$$

we have for the invariant two-particle energy  $s_{12} \equiv (k_1 + k_2)^2$

$$s_{12} - m_1^2 - m_2^2 = 2k_1 k_2 = 2(k_{10}k_{20} - k_{1z}k_{2z}) - 2(\mathbf{k}_1 \mathbf{k}_2)_\perp.$$

Transverse momenta do not change under the longitudinal Lorentz boost; the longitudinal part of the product of four-momenta depends on the difference of two rapidities (also an invariant)

$$(k_{10}k_{20} - k_{1z}k_{2z}) = m_{1\perp} m_{2\perp} \cosh(\eta_1 - \eta_2). \tag{9.53}$$

In terms of the rapidity, the particle phase space reads

$$\frac{d^3\mathbf{k}}{k_0} = d^2\mathbf{k}_\perp \frac{dk_z}{k_0} = d^2\mathbf{k}_\perp d\eta. \tag{9.54}$$

The property (9.45) translates then into *homogeneity* in rapidity. Let us introduce rapidities of the colliding particles,

$$\begin{aligned} \eta_+ &= \ln \frac{p_{10} + p_{1z}}{m} \simeq \ln \frac{2p_{10}}{m}, \\ \eta_- &= \ln \frac{p_{20} + p_{2z}}{m} = -\ln \frac{p_{20} - p_{2z}}{m} \simeq -\ln \frac{2p_{20}}{m}. \end{aligned} \tag{9.55}$$

Each of them depends, obviously, on the frame. For example, in the laboratory frame  $\eta_- = 0$ ,  $\eta_+ = \ln(s/m^2)$ ; in the centre-of-mass frame of the collision  $\eta_+ = -\eta_- = \frac{1}{2} \ln(s/m^2)$ , etc. preserving the invariant difference

$$\eta_+ - \eta_- \simeq \ln \frac{4p_{10}p_{20}}{m^2} = \ln \frac{s}{m^2}.$$

The Sudakov variables are invariants too and are linked to the rapidity as follows

$$\begin{aligned} k &= \beta p'_1 + \alpha p'_2 + k_\perp; \\ \beta &= \sqrt{\frac{k^2 + \mathbf{k}_\perp^2}{s}} \exp\left\{ \eta - \frac{1}{2}(\eta_+ + \eta_-) \right\}, \\ \alpha &= \sqrt{\frac{k^2 + \mathbf{k}_\perp^2}{s}} \exp\left\{ -\eta + \frac{1}{2}(\eta_+ + \eta_-) \right\}. \end{aligned} \tag{9.56}$$

In terms of rapidities (9.44) simplifies. Introducing an additional  $\mathbf{k}_\perp$  integration, we can represent the particle distribution in an exceptionally

simple symmetric form:

$$\begin{aligned} \sigma_{n+2} = & \frac{\sigma_2(s)}{\beta(0)} \prod_{i=0}^{n+1} \left( \int \frac{d^2\mathbf{k}_{i\perp}}{2(2\pi)^3} \int d\eta_i \right) \cdot \prod_{i=1}^{n+1} \frac{g^2}{[m^2 + \mathbf{q}_{i\perp}^2]^2} \\ & \times 2(2\pi)^3 \delta^{(2)} \left( \sum_{i=0}^{n+1} \mathbf{k}_{i\perp} \right) \delta(\eta_0 - \eta_+) \delta(\eta_{n+1} - \eta_-), \end{aligned} \tag{9.57a}$$

where the ordering of rapidities is implied,

$$\eta_+ = \eta_0 > \eta_1 > \eta_2 > \dots > \eta_n > \eta_{n+1} = \eta_- . \tag{9.57b}$$

In (9.57a)  $\mathbf{q}_{i\perp}$  are transverse momenta of the vertical lines,

$$\mathbf{q}_{i\perp} = \sum_{m=0}^{i-1} \mathbf{k}_{m\perp} . \tag{9.57c}$$

The only dependence on rapidities is contained in the ordering condition (9.57b); otherwise, the multi-particle distribution given by the integrand of (9.57a) depends only on the transverse momenta.

### 9.3.5 Rapidity plateau in the inclusive spectrum

The homogeneity of the particle distribution in rapidity is of extreme importance for the Regge-pole picture. How to verify this property experimentally? Let us look at the inclusive production cross section of a particle with momentum  $\eta$ ,  $\mathbf{k}_{\perp}$ . We need to integrate the cumbersome expression (9.57a) over the variables of all particles but one,

$$\sigma_{n+2} \equiv \int d^2k_{\perp} d\eta f_n(k_{\perp}, \eta), \tag{9.58a}$$

and construct the sum

$$\frac{d\sigma}{d^2\mathbf{k}_{\perp} d\eta} = f(k_{\perp}, \eta) \equiv \sum_n f_n(k_{\perp}, \eta). \tag{9.58b}$$

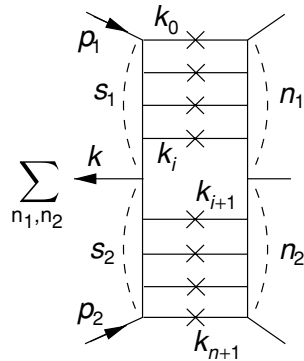
As we have just discussed above, it is normalized as follows,

$$\sum_n \int d^2k_{\perp} d\eta f_n(k_{\perp}, \eta) = \sum_n n \sigma_{n+2} = \bar{n} \cdot \sigma_{\text{tot}}, \tag{9.59}$$

where  $\bar{n}$  is the average number of particles produced *in addition* to the two leading ones. If one includes the end points  $\eta = \eta_{\pm}$  in the rapidity integration in (9.59), then  $\bar{n}$  will be by two units bigger and count all the particles in the event.

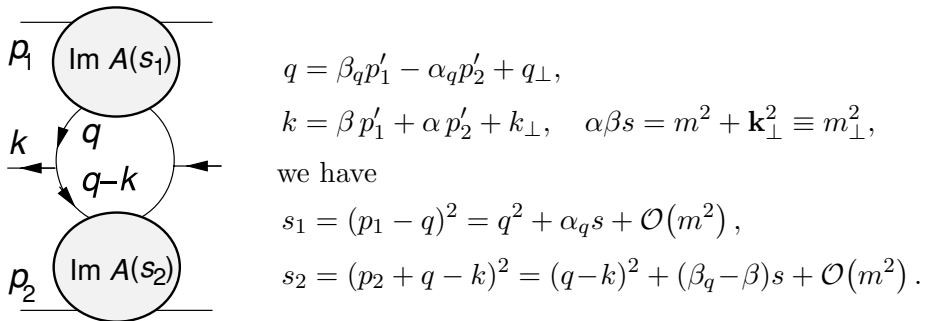
We calculate now the inclusive cross section in perturbation theory.

We take the imaginary part of the forward scattering amplitude and choose one particle somewhere in the middle of the ladder, not too close in rapidity to the leaders. Above and below the selected rung there will be two shorter ladders again. Integrating over loop momenta inside these two ladders and summing over  $n_1$  and  $n_2$  results in the appearance of the product of the imaginary parts of two new forward amplitudes, and we get



$$2(2\pi)^3 f(k) = \frac{1}{j} \int \frac{d^4q}{(2\pi)^3} \frac{1}{[m^2 - q^2]^2} \frac{1}{[m^2 - (q - k)]^2} \cdot 2 \operatorname{Im} A((p_1 - q)^2, q^2) \cdot 2 \operatorname{Im} A((p_2 + q - k)^2, (q - k)^2). \tag{9.60}$$

Let us evaluate the invariants entering the two blocks. Casting the momenta in the Sudakov basis as



Let us express the longitudinal integration variables  $\alpha_q$  and  $\beta_q$  in units of  $\alpha, \beta$  by introducing the fractions  $z_1, z_2 > 0,$

$$\alpha_q \equiv z_1 \cdot \alpha, \quad (\beta_q - \beta) \equiv z_2 \cdot \beta \quad (\beta_q = (1 + z_2)\beta);$$

$$d\alpha_q d\beta_q \frac{s}{2} = dz_1 dz_2 \frac{m_\perp^2}{2}. \tag{9.61}$$

Then the momenta squared read

$$-q^2 \sim \alpha_q \beta_q s = z_1(1 + z_2)m_\perp^2,$$

$$-(q - k)^2 \sim (\alpha_q + \alpha)(\beta_q - \beta)s = (1 + z_1)z_2 m_\perp^2, \tag{9.62}$$

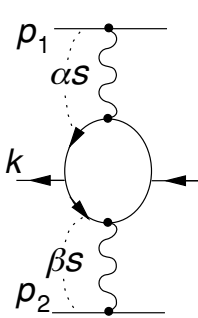
where we have combined the product  $\alpha\beta$  into the transverse mass.

The virtualities in (9.60) are limited. Therefore from (9.62) follows that  $z_i$  cannot run large. This tells us that the invariant energies of the two

blocks are practically fixed by the parameters of the registered particle  $k$ ,

$$\begin{aligned} s_1 &\simeq \alpha_q s \equiv \alpha s \cdot z_1, & z_1 &\sim 1; \\ s_2 &\simeq (\beta_q - \beta)s \equiv \beta s \cdot z_2, & z_2 &\sim 1. \end{aligned} \tag{9.63}$$

We conclude that both blocks are in the asymptotic regime,  $s_1, s_2 \gg m^2$ , so that we can substitute the Regge pole amplitudes, see (9.40a),



$$\text{Im } A^{\text{pole}}(p_1, q) = g^2 \pi \beta(0) \left( \frac{s_1}{m^2} \right)^{\alpha(0)},$$

$$\text{Im } A^{\text{pole}}(p_2, q - k) = g^2 \pi \beta(0) \left( \frac{s_2}{m^2} \right)^{\alpha(0)}.$$

In these blocks the  $s$ -dependence of the inclusive cross section is hidden; neither the propagators in (9.60) nor the phase space (9.61) contain  $s$ . The partial energies  $s_1$  and  $s_2$  in (9.63) obviously depend on the particle rapidity,

$$s_1 \sim \alpha s = m_{\perp} \sqrt{s} e^{-(\eta - \bar{\eta})}, \quad s_2 \sim \beta s = m_{\perp} \sqrt{s} e^{\eta - \bar{\eta}}; \quad \bar{\eta} \equiv \frac{1}{2}(\eta_+ + \eta_-),$$

but in their product this dependence disappears,

$$\left( \frac{s_1}{m^2} \frac{s_2}{m^2} \right)^{\alpha(0)} = \left( \frac{s}{m^2} \right)^{\alpha(0)} \cdot \left( z_1 z_2 \frac{m_{\perp}^2}{m^2} \right)^{\alpha(0)}.$$

Taken together with the flux factor,  $j^{-1} \simeq s^{-1}$ , we reproduce the  $s$ -behaviour of  $\sigma_{\text{tot}}(s)$  (9.40a). This being the only  $s$ -dependent ingredient of (9.60), for the inclusive cross section we finally obtain

$$f(k_{\perp}, \eta) = \sigma_{\text{tot}}(s) \cdot \phi(\mathbf{k}_{\perp}^2), \tag{9.64}$$

where the normalized inclusive spectrum  $\phi$  depends neither on  $s$  nor on the rapidity  $\eta$  of the triggered particle. The spectrum density  $\phi$  has the following structure

$$\begin{aligned} \phi(\mathbf{k}_{\perp}^2) &\propto (m_{\perp}^2)^{\alpha(0)+1} \int d^2 \mathbf{q}_{\perp} \int_0^{\infty} dz_1 z_1^{\alpha(0)} \int_0^{\infty} dz_2 z_2^{\alpha(0)} \\ &\cdot \frac{1}{[m^2 + \mathbf{q}_{\perp}^2 + z_1(1+z_2)m_{\perp}^2]^2 [m^2 + (\mathbf{q} - \mathbf{k})_{\perp}^2 + (1+z_1)z_2 m_{\perp}^2]^2}. \end{aligned} \tag{9.65}$$

Its normalization is easy to fix using the general relation (9.59),

$$\begin{aligned} \int_{\eta_-}^{\eta_+} d\eta \int d^2 \mathbf{k}_{\perp} f(k_{\perp}, \eta) &= \bar{n}(s) \cdot \sigma_{\text{tot}} = \beta(0) \ln \frac{s}{m^2} \cdot \sigma_{\text{tot}}, \\ \implies \int d^2 \mathbf{k}_{\perp} \phi(\mathbf{k}_{\perp}^2) &= \beta(0). \end{aligned} \tag{9.66}$$



In the spirit of the Regge pole picture, the inclusive spectrum  $f(k_{\perp}, \eta)$  can be represented graphically as

$$f(k_{\perp}, \eta) = \text{Diagram} \tag{9.67}$$

where  $\phi$  plays the rôle of a new reggeon–reggeon vertex with the production of the particle with a given  $\mathbf{k}$ .

One can study multi-particle observables as well. Consider, for example, the double inclusive cross section,  $f(k_1, k_2)$ , which characterizes the production of two particles with fixed momenta in the same event. The consideration analogous to (9.51) which has led us to the normalization of the one-particle inclusive cross section,

$$\frac{1}{\sigma_{\text{tot}}} \int f(k_1) d\Gamma(k_1) = \bar{n}, \tag{9.68a}$$

yields in the case of two registered particles

$$\frac{1}{\sigma_{\text{tot}}} \int d\Gamma(k_1) d\Gamma(k_2) f(k_1, k_2) = \langle n(n-1) \rangle = \langle n^2 \rangle - \bar{n}. \tag{9.68b}$$

To see whether particles are correlated, one constructs the difference

$$C_2(k_1, k_2) = \frac{f(k_1, k_2)}{\sigma_{\text{tot}}} - \frac{f(k_1)}{\sigma_{\text{tot}}} \frac{f(k_2)}{\sigma_{\text{tot}}}.$$

The phase space integral of the correlation function,

$$\int d\Gamma(k_1) d\Gamma(k_2) C_2(k_1, k_2) = (\langle n^2 \rangle - \bar{n}^2) - \bar{n},$$

is zero for the Poisson distribution.

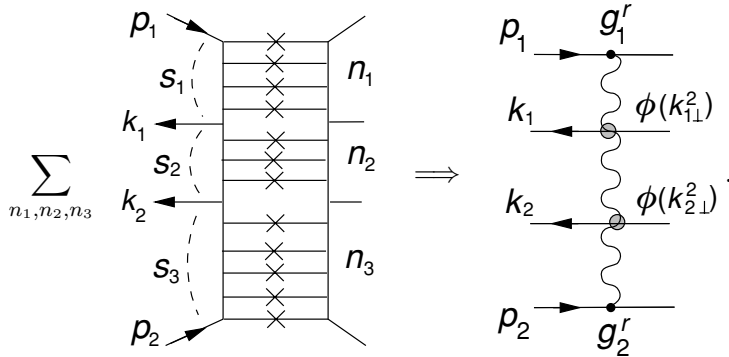
We take the ladders and assemble the intermediate lines into three Regge pole amplitudes, provided the pair energies are large. Invoking the kinematical relation (9.50),

$$(s_1 s_2 s_3)^{\alpha(0)} = s^{\alpha(0)} (m^2 + \mathbf{k}_{1\perp}^2)^{\alpha(0)} (m^2 + \mathbf{k}_{2\perp}^2)^{\alpha(0)},$$

we arrive at

$$f(k_1, k_2) = f(\mathbf{k}_{1\perp}, \eta_1; \mathbf{k}_{2\perp}, \eta_2) = s^{\alpha(0)-1} g_1^r \phi(\mathbf{k}_{1\perp}^2) \phi(\mathbf{k}_{2\perp}^2) g_2^r. \quad (9.69)$$

In a full analogy with (9.67) the double inclusive cross section does not depend on particle rapidities. In perturbation theory particles (with large relative rapidity) are produced independently,  $C_2(k_2, k_2) \equiv 0$ .



The fact that the inclusive cross sections do not depend on rapidity looks very natural; in the first place, there was no  $\eta_i$  dependence in the underlying multi-particle distribution (9.57) either. On the other hand, if we have indeed a Regge pole, it could not possibly be otherwise.

We have said before that the pole is *factorized*. This means that after a few steps away from the leading particle (say, descending the ladder) the system goes over into a definite state which no longer ‘remembers’ about the initial state, about the quantum numbers of the projectile and, in particular, about the initial momentum. But how can this be possible?

Let us change the reference frame by moving along the collision axis with some velocity  $v$  corresponding to  $\Delta\eta$  in rapidity. Then the distribution  $f(\eta)$  will shift as a whole,  $f \rightarrow f(\eta + \Delta\eta)$ . But if the particle deep inside the ‘ladder’ has forgotten about the energies of the colliding particles  $p_1$  and  $p_2$  (factorization!), then the probability to observe the particle should not change. (We cannot say much about the edges of the distribution,  $\eta \simeq \eta_{\pm}$ , at the moment. We will discuss this issue in what follows.)

Thus the uniformity in rapidity – the so-called *rapidity plateau* – is just the consequence of the factorization. We shall see later that homogeneity in rapidity follows from the factorization also beyond the perturbation theory, if the average transverse momentum of hadrons does not increase with the energy  $s$ .

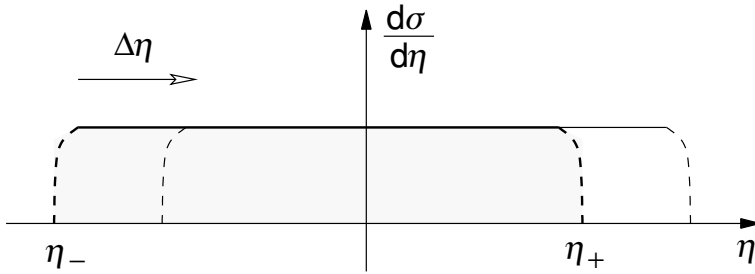


Fig. 9.6 Plateau in the inclusive cross section. Changing the reference frame does not affect particle density inside the ladder.

The mean particle multiplicity increases with the width of the distribution,  $\eta_+ - \eta_- = \ln(s/m^2)$ , in Fig. 9.6. The height equals  $\beta(0) \propto \bar{g}^2$ ; in the perturbation theory it is small.

9.3.6 Particle distribution in the impact parameter space

The impact parameters of colliding particles do not change in the course of the high-energy scattering. And how are the *newly produced* particles distributed in the impact parameter space? Answering this question will allow us to understand the origin of the impact parameter structure of the pomeron amplitude (8.22):

$$\text{Im } A^{\text{pole}}(s, \rho_{12}) = \frac{1}{4\pi\alpha'\xi} \exp \left\{ -\frac{(\rho_1 - \rho_2)^2}{4\alpha'\xi} \right\}, \quad \xi = \ln \frac{s}{m^2}. \quad (9.70)$$

In Lecture 5 we speculated about the possibility of having the interaction radius growing with energy. We saw that the random walk in the impact parameter, due to long-living multi-particle fluctuations, is capable of generating the growth of the radius characteristic for the Regge pole exchange (9.70), namely  $\rho \propto \sqrt{\xi}$ . Now we are in a position to verify this expectation within our perturbative model.

Take the ladder amplitude,

$$\begin{aligned} f(\mathbf{k}_0; \mathbf{k}_1, \dots, \mathbf{k}_n; \mathbf{k}_{n+1}) &= g^{n+2} \frac{1}{m^2 + \mathbf{k}_{0\perp}^2} \frac{1}{m^2 + (\mathbf{k}_0 + \mathbf{k}_1)_\perp^2} \dots \\ &\dots \frac{1}{m^2 + (\mathbf{k}_1 + \dots + \mathbf{k}_{n-1})_\perp^2} \frac{1}{m^2 + (\mathbf{k}_1 + \dots + \mathbf{k}_n)_\perp^2} \\ &= g^n \frac{1}{m^2 + \mathbf{q}_{1\perp}^2} \frac{1}{m^2 + \mathbf{q}_{2\perp}^2} \dots \frac{1}{m^2 + \mathbf{q}_{n,\perp}^2} \frac{1}{m^2 + \mathbf{q}_{n+1,\perp}^2}, \end{aligned} \quad (9.71)$$

and Fourier-transform it to the impact parameter space,

$$f(\boldsymbol{\rho}_0, \boldsymbol{\rho}_1, \dots, \boldsymbol{\rho}_{n+1}) = \int \frac{d^2 \mathbf{k}_{1\perp}}{(2\pi)^2} \dots \frac{d^2 \mathbf{k}_{n\perp}}{(2\pi)^2} e^{i \sum_{i=0}^{n+1} (\mathbf{k}_i \cdot \boldsymbol{\rho}_i)} f(\mathbf{k}_0, \dots, \mathbf{k}_{n+1}),$$

where the integral over the last transverse momentum,  $\mathbf{k}_{n+1,\perp}$  was traded for the momentum-conservation condition,  $\delta^2(\sum_{i=0}^{n+1} \mathbf{k}_{i\perp})$ . The Fourier exponent can be cast in terms of the transferred momenta  $\mathbf{q}_i$ ,

$$\sum_{i=0}^{n+1} \mathbf{k}_i \cdot \boldsymbol{\rho}_i = \mathbf{q}_1 \cdot (\boldsymbol{\rho}_0 - \boldsymbol{\rho}_1) + \mathbf{q}_2 \cdot (\boldsymbol{\rho}_1 - \boldsymbol{\rho}_2) + \dots + \mathbf{q}_{n+1} \cdot (\boldsymbol{\rho}_n - \boldsymbol{\rho}_{n+1}).$$

Then, given the factorized structure of (9.71) in  $\mathbf{q}_i$ , the transformed amplitude comes out very simple,

$$f(\boldsymbol{\rho}_0, \dots, \boldsymbol{\rho}_{n+1}) = g^{n+2} \varphi(\boldsymbol{\rho}_0 - \boldsymbol{\rho}_1) \varphi(\boldsymbol{\rho}_1 - \boldsymbol{\rho}_2) \dots \varphi(\boldsymbol{\rho}_n - \boldsymbol{\rho}_{n+1}), \quad (9.72a)$$

$$\varphi(\boldsymbol{\rho}) = \int \frac{d^2 \mathbf{q}}{(2\pi)^2} \frac{e^{i \mathbf{q} \cdot \boldsymbol{\rho}}}{m^2 + \mathbf{q}^2}. \quad (9.72b)$$

The probability of a given configuration will be given by  $|f(\boldsymbol{\rho}_1, \dots, \boldsymbol{\rho}_n)|^2$ . Integration of the squared amplitude over all impact parameters  $\boldsymbol{\rho}_i$  will obviously produce the ladder cross section  $\sigma_n$ .

Consider the probability  $w_{\tau, \tau'}(\boldsymbol{\rho})$  of finding two particles, labelled  $\tau$  and  $\tau'$  at some distance  $|\boldsymbol{\rho}|$ . This is a typical *inclusive* characteristic: we don't restrict other particles and integrate over their position in the transverse plane. The chain structure of the amplitude (9.72a) makes it clear that the positions of the ladder rungs with numbers  $i$  *outside* the interval between the triggered particles,  $i \notin [\tau, \tau']$ , will be integrated out freely without affecting the answer.

We can pick, for example, the last rung,  $\tau' = n + 1$ , and since the answer depends only on the difference of the coordinates, set  $\boldsymbol{\rho}_{n+1} = \mathbf{0}$ . This way we will be studying the distance of the particle  $\tau$  from the target  $p_2$ .

The normalized probability takes the form

$$w_{\Delta}(\boldsymbol{\rho}) = \frac{1}{N\Delta} \int d^2 \boldsymbol{\rho}_{\tau+1} \dots d^2 \boldsymbol{\rho}_n \varphi^2(\boldsymbol{\rho} - \boldsymbol{\rho}_{\tau+1}) \varphi^2(\boldsymbol{\rho}_{\tau+1} - \boldsymbol{\rho}_{\tau+2}) \dots \varphi^2(\boldsymbol{\rho}_n),$$

$$\Delta = n + 1 - \tau; \quad \int d^2 \boldsymbol{\rho} w_{\Delta}(\boldsymbol{\rho}) = 1, \quad N \equiv \int d^2 \boldsymbol{\rho} \varphi^2(\boldsymbol{\rho}). \quad (9.73)$$

The integrand of  $w_{\Delta}$  contains  $\Delta$  factors  $\varphi$ ; the number of integrations is  $\Delta - 1$ . In one step from the target,  $\tau = n$ , we have the probability  $w_1(\boldsymbol{\rho}) = \varphi^2(\boldsymbol{\rho})$  given by (9.72b). At distances larger than the characteristic radius  $r_0 = m^{-1}$  it falls exponentially,  $\varphi(\boldsymbol{\rho}) \sim \exp(-|\boldsymbol{\rho}|/r_0)$ . It is natural

to expect that with the number of steps  $\Delta$  increasing, the probability of finding the particle will spread.

Indeed, (9.73) is a typical diffusion problem with  $\varphi^2(\boldsymbol{\rho})$  the probability distribution of ‘jumping’ at a distance  $\sim r_0$ ; the convolution (9.73) describes the result after  $\Delta$  independent jumps. Whatever the form of the initial distribution  $w_1$ , after a few jumps  $w_\Delta(\boldsymbol{\rho})$  becomes a *Gaussian*. Let us find its *dispersion*  $\sigma_\Delta$ ,

$$w_\Delta(\boldsymbol{\rho}) \simeq \frac{1}{\pi\sigma_\Delta^2} \exp\left\{-\frac{\boldsymbol{\rho}^2}{\sigma_\Delta^2}\right\}, \tag{9.74a}$$

which measures the average squared distance from the target,

$$\sigma_\Delta^2 = \langle \boldsymbol{\rho}^2 \rangle_\Delta = \int d^2\boldsymbol{\rho}_\tau \int dw_\Delta(\boldsymbol{\rho}_\tau) \left( \sum_{k=1}^\Delta [\boldsymbol{\rho}_{\tau+k-1} - \boldsymbol{\rho}_{\tau+k}] \right)^2. \tag{9.74b}$$

Since the directions of individual jump are uncorrelated, averaging the squared sum yields simply

$$\langle \boldsymbol{\rho}^2 \rangle_\Delta = \Delta \cdot \langle \boldsymbol{\rho}^2 \rangle_1, \tag{9.75a}$$

$$\langle \boldsymbol{\rho}^2 \rangle_1 = \int dw_1(\boldsymbol{\rho}) \boldsymbol{\rho}^2 = \frac{1}{N} \int d^2\boldsymbol{\rho} \varphi^2(\boldsymbol{\rho}) \cdot \boldsymbol{\rho}^2. \tag{9.75b}$$

To calculate the concrete number is of little interest. We will, instead, relate (9.75) directly to the Regge pole trajectory.

To do that, we go back for a moment to the momentum representation. From (9.72b) it immediately follows that the *Fourier image* of the probability distribution is nothing but the Regge trajectory,

$$\int d^2\boldsymbol{\rho} \varphi^2(\boldsymbol{\rho}) e^{-i\mathbf{q}\cdot\boldsymbol{\rho}} = \int \frac{d^2\mathbf{q}'}{(2\pi)^2} \frac{1}{[m^2 + \mathbf{q}'^2][m^2 + (\mathbf{q}' - \mathbf{q})^2]} = c\beta(\mathbf{q}^2),$$

so that

$$\int dw_1(\boldsymbol{\rho}) e^{-i\mathbf{q}\cdot\boldsymbol{\rho}} = \frac{\beta(\mathbf{q}^2)}{\beta(0)}. \tag{9.76a}$$

Now the calculation of (9.75b) is very simple:

$$\begin{aligned} \langle \boldsymbol{\rho}^2 \rangle_1 &= \left\{ (i\nabla_{\mathbf{q}})^2 \int dw_1(\boldsymbol{\rho}) e^{-i\mathbf{q}\cdot\boldsymbol{\rho}} \right\}_{\mathbf{q}=0} \\ &= -\frac{4}{\beta(0)} \frac{d}{d\mathbf{q}^2} \beta(\mathbf{q}^2) \Big|_{\mathbf{q}=0} = 4 \frac{\alpha'(0)}{\beta(0)}, \end{aligned} \tag{9.76b}$$

where  $\alpha' = \beta'$  denotes the derivative of the trajectory over  $t = -\mathbf{q}^2$ .

Finally, what is the meaning of  $\Delta$  in (9.75a)? The number of particles we can evaluate as the size of the rapidity interval between the triggered particles, the particle  $\tau$ , and the target, multiplied by the average density of the plateau:

$$\sigma_{\Delta}^2 = \Delta \cdot \langle \rho^2 \rangle_1 = [(\eta - \eta_-) \times \beta(0)] \cdot 4 \frac{\alpha'}{\beta(0)}.$$

Substituting this dispersion into (9.75) and setting  $\eta = \eta_+$  we obtain exactly the impact parameter profile of the vacuum pole (9.70):

$$w_{\Delta}(\rho_{12}) \simeq \frac{1}{4\pi\alpha'\xi} \exp\left\{-\frac{\rho_{12}^2}{4\alpha'\xi}\right\} = A^{\text{pole}}(s, \rho_{12}). \tag{9.77}$$

### 9.3.7 Perturbative conclusions

Here we summarize the characteristic features of the inelastic processes which determine the Regge pole in perturbation theory.

- (1) Topological cross sections follow the Poisson distribution

$$\sigma_n(s) = \sigma_{\text{tot}}(s) \frac{[\bar{n}(s)]^n}{n!} e^{-\bar{n}(s)}. \tag{9.78a}$$

- (2) The mean particle multiplicity grows logarithmically with energy,

$$\bar{n}(s) = \beta(0)\xi, \quad \xi = \eta_+ - \eta_- = \ln \frac{s}{m^2}. \tag{9.78b}$$

- (3) The inclusive particle spectrum is flat in rapidity (plateau) and does not depend on the total energy,

$$\frac{d^3n}{d^2\mathbf{k}_{\perp} d\eta} = \frac{f(\mathbf{k}_{\perp}^2, \eta; s)}{\sigma_{\text{tot}}(s)} = \frac{\text{---} \text{---} \text{---} \text{---}}{\text{---} \bullet \text{---} \text{---}} \Bigg/ \frac{\text{---} \bullet \text{---} \text{---} \text{---}}{\text{---} \bullet \text{---} \text{---} \text{---}} = \phi(\mathbf{k}_{\perp}^2). \tag{9.78c}$$

- (4) The production of particles with large rapidity intervals between them is uncorrelated,

$$\frac{d^6n}{d^2\mathbf{k}_{1\perp} d\eta_1 d^2\mathbf{k}_{2\perp} d\eta_2} = \frac{\text{---} \bullet \text{---} \bullet \text{---} \text{---}}{\text{---} \bullet \text{---} \bullet \text{---} \text{---}} \Bigg/ \frac{\text{---} \bullet \text{---} \text{---} \bullet \text{---}}{\text{---} \bullet \text{---} \text{---} \bullet \text{---}} = \phi(\mathbf{k}_{1\perp}^2)\phi(\mathbf{k}_{2\perp}^2). \tag{9.78d}$$

- (5) The particle density in the plateau is small,

$$\frac{dn}{d\eta} = \int d^2\mathbf{k}_\perp \phi(\mathbf{k}_\perp^2) = \beta(0) \sim \frac{g^2}{m^2} \ll 1. \quad (9.78e)$$

- (6) The energy increase of the interaction radius characteristic for the Regge-pole exchange is due to diffusion in the impact parameter space,

$$\rho_0(s) \sim \sqrt{\beta'(0)} \xi. \quad (9.78f)$$